Simplified Wheel Slip Modeling and Estimation for Omnidirectional Vehicles

Bastiaan Vandewal, Joris Gillis, Goele Pipeleers and Jan Swevers
MECO Research Team, Department of Mechanical Engineering, KU Leuven, Belgium
Core Lab DMMS-M, Flanders Make, Leuven, Belgium
Email: bastiaan.vandewal@kuleuven.be

***Abstract*—This paper presents the development of a low-complexity wheel slip-based vehicle model for an omnidirectional vehicle equipped with Mecanum wheels that is suited for optimal control. Augmenting a vehicle model with wheel slip properties allows for better trajectory tracking, while the reduced model complexity allows for manageable parameter estimation and motion planning with lower computation times. The wheel slip model and optimal motion planning are validated on an in-house developed omnidirectional vehicle for three different surfaces. The estimation procedure of the slip model parameters for these surfaces is discussed and the effective application of these models in optimal motion planning is demonstrated. The results encourage to use simplified wheel slip models in motion planning problems to keep the computation time low and to increase the position accuracy, which reduces the need for positional feedback and fast online motion replanning if slip would occur.**

***Index Terms*—motion planning, friction, parameter estimation, mobile robots**

I. Introduction

Planning trajectories is an important task for an Automated Guided Vehicle (AGV). Typically, a motion trajectory describes the desired pose of the vehicle (position and orientation) as a function of time. Motion planning can generally be formulated as an optimal control problem (OCP), which solves for the optimal vehicle pose and motor inputs (e.g. speed and steering angle) in order to minimize an objective (e.g. travelling time) and to avoid obstacles, given the system kinematics or dynamics and taking vehicle limitations (e.g. maximum velocity or acceleration) into account. Neglecting physical phenomena or vehicle properties in this model (e.g. inertia effects, road slope, dynamic weight transfer or wheel slip) can yield motion trajectories that can only be executed by the vehicle with a limited accuracy. In the worst case, this trajectory might even be impossible to execute. This can lead to unexpected and unwanted behavior (e.g. collisions with obstacles or drifting) and also complicates the predictability of the vehicle's movement by people in the neighborhood, which might be a serious safety hazard. Currently, most autonomous vehicles in industry plan their trajectories using kinematic vehicle models and are restricted in velocity and acceleration to avoid phenomena like wheel slip and to ensure safe operation, which increases the economic cost as the AGV needs more time to travel a certain distance.

This work has been carried out within the framework of Flanders Make's SBO project MultiSysLeCo (Multi-System Learning Control). Flanders Make is the Flemish strategic research centre for the manufacturing industry.

This paper presents a method to handle wheel slip for omnidirectional vehicles during motion planning. In the remaining part of this introduction we consecutively discuss the concept of omnidirectional motion, which can be accomplished with different wheels, the kinematic and dynamic vehicle models that are available in literature, the concept of wheel slip and how to properly model the forces between wheel and road. We also shortly discuss different possibilities to compensate for possible position errors if wheel slip occurs without modeling it explicitly.

Omnidirectional movement can be accomplished in many ways with different arrangements of either appropriately steered conventional wheels (e.g. active castor wheels) or special unsteered wheels (e.g. universal wheels and Mecanum wheels). These three different wheels can be seen in Fig. 1. This paper considers the motion planning for a vehicle equipped with four separately driven Mecanum wheels, which are, unfortunately, very susceptible to slippage. Vehicles with this type of wheels have been investigated often for industrial applications [1] and as educational platforms, due to their attractive properties and high maneuverability. Mecanum wheels also possess some drawbacks such as the complex wheel design, which causes additional vibrations, and obliquely oriented wheel/road contact forces. Bayar [2] discusses the effects of these contact forces on the performance of Mecanum wheeled vehicles and thoroughly investigates the influence of the curvature of the rollers on the contact forces.

(a) Castor wheel (b) Universal wheel (c) Mecanum wheel

Fig. 1: Three different types of wheels that allow omnidirectional movement. Pictures from [3]–[5].

Due to the wide range of possible wheel types (e.g. fixed, orientable, castor or Mecanum) and wheel arrangements for omnidirectional vehicles, a considerable number of both kinematic and dynamic vehicle models are available in literature and some of them assume the no-slip condition. If slip is

taken into account, multiple techniques could be used to estimate the model parameters. The following gives a very concise overview of possible models and estimation techniques, available in literature. The necessity of incorporating wheel slip in vehicle models for vehicles with over-actuated wheels, as is often the case for omnidirectional vehicles, is described by Gracia et al. [6]. They present a kinematic and dynamic modeling method for any kind of wheeled mobile robot with slip based on physical principles and the Lagrange formulation. De Villiers et al. [7] present a dynamic control model for Mecanum wheels without concerning wheel slip. Another dynamic model is presented by Williams et al. [8] for a vehicle equipped with three universal omnidirectional wheels, including surface slip and they also experimentally determine the coefficients of friction for this model. Gustafsson [9] estimates tire/road friction for normal tires using wheel slip computed from standard sensor signals and proposes to use a parametric model based on experimental results for different surfaces, like gravel, asphalt and snow. He also points out that wheel slip might be accurately estimated by comparing the wheel speed of driven and undriven wheels, although this does not apply for all-wheel driven vehicles. Han et al. [10] state that wheel slip is the main source of position errors of omnidirectional mobile robots with Mecanum wheels and they introduce a parameter adjustment in the kinematic vehicle model. Chen et al. [11], finally, estimate the amount of slip by recursive least squares estimation for a Mecanum-wheeled vehicle and account for it.

A wheel rolls on a planar surface without slipping, when the point at the wheel in contact with the ground is instantaneously stationary with respect to the ground. The wheel angular velocity and vehicle speed are directly related in this case. Slipping (in the case of acceleration) or skidding (in the case of braking) occurs if this condition is not met and the torque provided by the motor to the wheel will be transformed only partially into vehicle movement in this case, i.e. the friction between the floor surface and the rollers is too low to transfer all forces properly and wheel slip occurs. A tire model describes this interaction between a vehicle tire and the floor surface or road profile. The tire forces are calculated in the tire/ground plane and show highly nonlinear behavior with respect to the amount of wheel slip. A tire model is typically given as a mathematical equation characterized by some dimensionless parameters, of which some even without a physical interpretation. The tire/road friction coefficient is the most commonly used model parameter as it describes the maximum value that the traction force, normalized against the vehicle weight, can achieve on a given surface for any wheel slip value. Tire models, which show the relationship between the normalized force and the amount of wheel slip, are derived empirically and mostly describe steady-state properties (found under constant but nonmatching rotational and translational velocities) as they are found by curve-fitting from experimental data [12]. These models appear in different forms of which the following are most convenient and often semi-empirical; the interpolation of look-up tables, the Dugoff brush tire model [13], Pacejka's Magic formula [14] and all simplified models derived from these models. They differ in complexity and accuracy and, depending on the purpose (e.g. suspension behavior, wheel slip, vehicle handling), one might prefer one model above another. Although the previous described slip models only describe steady-state behavior, tire force generation is not an instantaneous phenomenon. Consequently, multiple transient tire models have been developed, which become more important when a vehicle is driven at the limits of its maneuvering capability. Transient tire force behavior is often described with a (first order) transfer function or defined by a dynamic tire friction model which attempts to capture the transient behavior of the tire forces under time-varying velocity conditions [15].

In general, there are two main techniques to handle wheel slip, which can also be combined at the same time, namely modeling wheel slip or correcting the errors that are caused by wheel slip. The latter avoids procedures to model wheel slip by error compensation techniques, e.g. by feedback control, and is typically based on position measurements at an adequate sampling rate. The amount of feedback needed to keep close to the trajectory will be significant in the case of excessive wheel slip and may even deteriorate the results as it could introduce additional wheel slip. Feedback control is often used as an error compensation strategy in literature, such as visual dead-reckoning [16] (as classical odometry is not possible due to the sensitivity to wheel slip) or position compensation with additional sensors (e.g. ultrasonic sensors indoors [17] or GPS outdoors [18]). Another compensating strategy could be Model Predictive Control (MPC) for its implicit position feedback. However, in this paper, we focus on improving the tracking accuracy by including the wheel slip dynamics while planning the vehicle motion, minimizing the necessity to adjust for unwanted behavior and without using feedback control.

This paper is structured as follows. Section II presents the vehicle under investigation and shows how this vehicle can be modeled kinematically. It also brings wheel slip into the equations by introducing a parametric slip model with low complexity. Section III describes the measurement setup and details how the parameters of the new traction model can be estimated. In order to improve the motion planning capabilities with this wheel slip model, Section IV discusses the motion planning algorithm and compares the optimized solution with the results found under the no-slip assumption. Additionally, some experimental results are discussed in this section. In Section V, conclusions are drawn and possible extensions suggested.

II. Modeling of Omnidirectional Vehicles

The proposed method will be demonstrated on a Mecanum-wheeled omnidirectional vehicle but can straightforwardly be extended to all other kinds of vehicle or wheels by small adaptions or simplifications of the method presented here. This section describes our holonomic robotic platform and the kinematic model that is typically used for this vehicle.

Afterwards, the wheel equations are defined and wheel slip is introduced in order to define the dynamic equations.

A. Holonomic Robotic Platform

The implementation and demonstration of the presented approach is done on two robotic platforms, in-house developed by Van Parys et al. [19] and as presented in Fig. 2. Each platform consists of four Mecanum wheels, each built with nine small rollers around the rim, directly connected to an independently driven, battery-powered DC motor. The rollers are assumed to rotate freely around their axes as they contact the ground. An Odroid XU4 is the onboard computer that performs the motion planning and pose control. Communication from a remote device is possible through a Wi-Fi dongle. A micro-controller implements the low-level velocity control of the four DC motors and interfaces the encoders and IMUs. As there is no suspension system foreseen, wheel/road contact cannot be guaranteed at all time instances. Small irregularities or an unevenness of the ground surface might lead to additional inaccuracies, which will not be considered.

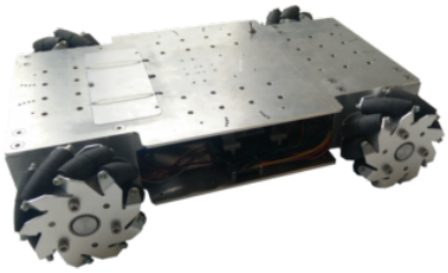

Fig. 2: In-house developed holonomic robotic platform.

B. Vehicle Model - Kinematics

The pose of the vehicle can be expressed in a fixed reference frame with three variables x, y and heading θ, which can be combined as the robot's pose $\boldsymbol{p} \in \mathbb{R}^3$. The corresponding first-order time derivative is given by $\dot{\boldsymbol{p}} = [v_x, v_y, \omega_z]^\top$ [20]. The kinematic vehicle model of a Mecanum-wheeled omnidirectional vehicle, with rollers at an angle of $\pm 45°$ to the rotational plane, is typically given by the following relationship between the independent angular wheel speeds $\dot{\varphi}_i$ and the vehicle speed $\dot{\boldsymbol{p}}$ with r the radius of the wheel (5 cm) and l and w half of the length (40 cm) and width (30 cm) of the wheelbase respectively [21]:

$$\begin{bmatrix} \dot{\varphi}_1 \\ \dot{\varphi}_2 \\ \dot{\varphi}_3 \\ \dot{\varphi}_4 \end{bmatrix} = \frac{1}{r} \begin{bmatrix} 1 & 1 & -l-w \\ -1 & 1 & l+w \\ -1 & 1 & -l-w \\ 1 & 1 & l+w \end{bmatrix} \begin{bmatrix} v_x \\ v_y \\ \omega_z \end{bmatrix}. \tag{1}$$

All these variables and parameters are indicated on Fig. 4. Vehicles equipped with omnidirectional wheels allow for special maneuverability since it allows both translational mobility in all directions, as well as rotational mobility. Rotational movement will not be considered further on, as we limit ourselves to movements with a fixed heading, i.e. $\omega_z = 0$.

TABLE I: Variables used in the wheel equations.

Symbol	Unit	Description
$\boldsymbol{v}_{\text{slip}\,i}$	m/s	sliding velocity vector of wheel i
α_i	rad	angular coordinate of wheel i in the vehicle frame
γ_i	rad	orientation of rollers of wheel i ($\pm 45°$)
d	m	distance between wheel and vehicle center
r	m	wheel radius
r_r	m	roller radius
$\dot{\varphi}_i$	rad/s	rotation velocity of wheel i
$\dot{\varphi}_{ri}$	rad/s	rotation velocity of the roller of wheel i
$\dot{\boldsymbol{p}}$		vehicle velocity in the world frame; $[v_x, v_y, \omega_z]^\top$
m	kg	vehicle mass

C. Wheel Equations and Wheel Slip

Gracia [22] developed kinematic wheel equations, expressing the sliding velocity vector, for different types of wheels using a vector approach of which the following equation represents the one for a vehicle with Mecanum wheels, aligned with the vehicle and expressed in a coordinate frame connected to and directed along the roller, and where we have used the variables of Table I:

$$\boldsymbol{v}_{\text{slip}\,i} = \begin{bmatrix} \mathbf{R} & \begin{matrix} r_i \sin(\gamma_i) & 0 \\ r_i \cos(\gamma_i) & r_{ri} \end{matrix} \end{bmatrix} \times \begin{bmatrix} \dot{\boldsymbol{p}} \\ \dot{\varphi}_i \\ \dot{\varphi}_{ri} \end{bmatrix}, \tag{2}$$

with

$$\mathbf{R} = \begin{bmatrix} \cos(\gamma_i) & \sin(\gamma_i) & d_i \sin(\gamma_i - \alpha_i) \\ -\sin(\gamma_i) & \cos(\gamma_i) & d_i \cos(\gamma_i - \alpha_i) \end{bmatrix}. \tag{3}$$

As discussed by Muir [23], it is important to include the concept of wheel slip at an early stage of modeling as it is very difficult to fit wheel slip in existing models that start from the no-slip assumption. By enforcing zero wheel slip, i.e. $\boldsymbol{v}_{\text{slip}\,i} = 0\ m/s$, in this equation, it could be directly simplified to one of the wheel equations of (1). Since the rotation velocity of the free rollers $\dot{\varphi}_{ri}$ is uncontrolled and unknown, only the first row of (2) can be used in practice and the vector $\boldsymbol{v}_{\text{slip}\,i}$ becomes a scalar value $v_{\text{slip}\,i}$. Additionally, we assume that there will be no slip in the rolling direction since the roller can rotate freely. Hence, all forces will be directed perpendicular to the rolling direction of the free rollers.

The amount of wheel slip, v_{slip}, also referred to as the wheel relative velocity or sliding velocity, boils down to the difference between the surface speed of the wheel, based on the rotational wheel velocity $\dot{\varphi}$, and the translational velocity of the wheel center v. For a standard wheel with fixed orientation in the longitudinal direction, this is written as:

$$v_{\text{slip}} = r\dot{\varphi} - v_y. \tag{4}$$

Consequently, the longitudinal slip ratio, also known as the slip coefficient τ, is mostly defined as:

$$\tau = \begin{cases} \dfrac{v_{\text{slip}}}{r\dot{\varphi}}, & \text{if } r\dot{\varphi} \geq v_y \quad \text{(acceleration)}, \\ \dfrac{v_{\text{slip}}}{v_y}, & \text{if } r\dot{\varphi} < v_y \quad \text{(braking)}. \end{cases} \tag{5}$$

Tire friction models describe a normalized tire friction coefficient μ, defined as the ratio of friction force to normal

force. Usually, this is done by a highly nonlinear relationship as stated in Section I, e.g. the Magic Formula, as can be seen in Fig. 3 for different road surface conditions [15]. Direct use of these existing friction models entails multiple drawbacks or difficulties. A main drawback of these models is the fact that they only describe steady-state force as a function of slip ratio. These conditions are never met during driving conditions as both velocities, wheel and vehicle velocity, cannot be controlled individually. A second drawback, specifically for the Magic Formula, is the large number of parameters involved, making it difficult to conveniently identify them, and the nonlinearities with tedious trigonometric functions. This makes these friction models impractical or even useless for online optimal control, as discussed by Canudas-de-Wit et al. [15].

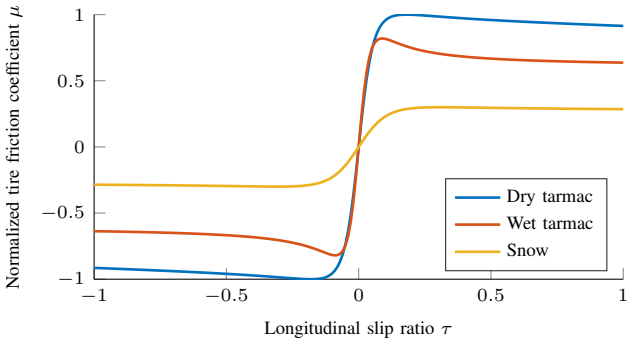

Fig. 3: Classical variation of tire/road friction profiles for different road surface conditions.

Another difficulty with road/tire friction modeling based on the slip ratio, is the varying definition of the longitudinal slip ratio to distinguish the cases of acceleration and braking, as can be seen in (5). A fourth issue entails an undefined slip ratio if either the vehicle or a wheel is standing still. To cope with these issues, we propose to use a formulation, which is suited to be implemented in an optimal control problem (OCP) by introducing a simplified continuously differentiable friction or traction model such as a hyperbolic tangent function, as done previously by Stepanyuk et al. [24]. This model is expressed as a function of the wheel's relative velocity v_{slip} as defined above. This directly solves all described difficulties and, by proper model choice, uses only two model parameters w_1 and w_2, related to the maximum friction coefficient and the slope of the coefficient in the low slip velocity region:

$$\mu_i = w_1 \tanh(w_2 v_{\text{slip}\,i}) \text{ for } i = (1...4). \tag{6}$$

As such, we mainly focus on the dependency of two physical entities for the friction coefficient, the wheel slip on the one hand and a quantity that incorporates the surface roughness and wheel material on the other hand. This (artificial) model should capture the most important friction characteristics and approximates all combined friction effects, without being too complex to be implemented in a motion planning algorithm.

D. Vehicle Model - Dynamics

Fig. 4 illustrates the traction forces that will enable acceleration of our vehicle for the chosen configuration of wheels. The rotating wheel will exert a force F_i along the roller's axis, perpendicular to the rolling direction. The contact point between the roller and the ground moves as the wheel rotates from one side of the wheel to the other. This displacement might introduce additional vibrations and unmodeled vehicle movement, but is neglected for simplicity. The summation of all these individual wheel forces, which depend on the wheel relative velocity of each wheel, produces a total force which can be in any direction. As such it allows the vehicle to move in any desired direction.

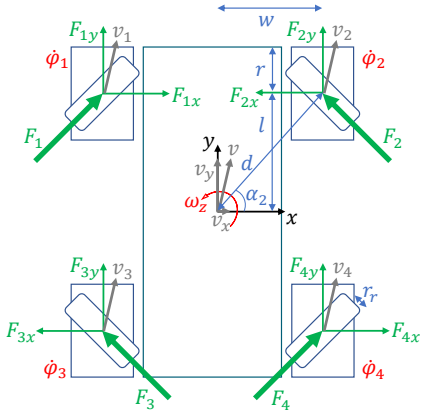

Fig. 4: Sketch of the vehicle with all contact forces between vehicle and floor.

Combining all these equations and assumptions yields the following procedure to calculate the expected vehicle velocity, given the individual wheel speeds and current vehicle velocity. Firstly, we calculate the amount of wheel slip, $v_{\text{slip}\,i}$, for each wheel independently based on (2). Secondly, we calculate the transferable force F_i based on the traction coefficient for this specific amount of wheel slip for every wheel by using our friction model (6) and the normal force;

$$F_i = \frac{mg}{4}\mu_i(v_{\text{slip}\,i}) \text{ for } i = (1...4). \tag{7}$$

Then, all these forces are projected and summed to yield the total amount of force in both directions;

$$\begin{aligned} F_x &= \cos\left(\frac{\pi}{4}\right)(F_1 - F_2 - F_3 + F_4), \\ F_y &= \sin\left(\frac{\pi}{4}\right)(F_1 + F_2 + F_3 + F_4). \end{aligned} \tag{8}$$

As we do not allow any rotational movement of the vehicle ($\dot{\theta} = 0$), the resulting moment of these forces should be zero. Finally, these forces can be integrated to compute the new vehicle velocity and, if needed, coordinates of the vehicle, based on the following relationship, after which this procedure can be repeated:

$$\begin{aligned} \dot{v}_x &= \frac{F_x}{m}, \\ \dot{v}_y &= \frac{F_y}{m}. \end{aligned} \tag{9}$$

While following this procedure, we assume that we control the wheel velocities and not the wheel torques. Hence, the wheel motor torques are not included in our model and we can directly use the wheel velocities as input variables of our model. However, as there might be a discrepancy between the requested and actually realized wheel velocities (as can be read from the wheel encoders), this should also be taken into account for motion planning purposes later on. Some small experiments indicated that the relationship between the desired and realized wheel speeds is approximately a first order system, which will be included while planning the trajectories.

III. Estimation of Wheel Slip Parameters

The friction model requires knowledge or estimates of the previously defined friction parameters w_1 and w_2. The procedure to estimate these values boils down to estimating the amount of traction force during a specific vehicle movement based on accurate measurements from both the wheel encoders and a global vehicle position and orientation measurement, e.g. a camera system, to get the wheel velocities and vehicle velocity respectively.

A. Measurement Setup

The trajectory of the vehicle is measured by tracking markers using a Krypton K600 vision system from NIKON Metrology, as illustrated in Fig. 5. The volumetric (static) accuracy of this measurement system changes with the distance to the camera and is given as 90 μm + 25 μm/m in the region of interest (measured between a distance of 3.5 to 5 m from the camera) [25]. Three noncollinear infrared light active markers, represented by m_1, m_2 and m_3, are attached to the AGV at fixed locations. Any led in the field of view of the system is identified by three calibrated linear CCD cameras, after which the position of every LED in 3D space is determined through triangulation at a rate of 100 Hz in the camera frame $\{k\}$.

The spatial position of the vehicle in 2D space, represented by an orthogonal frame $\{v\}$, registering the frame's orientation and position and expressed with respect to the world reference frame $\{w\}$, has to be determined from the position measurements of the LED markers unambiguously. As stated previously, these measurements are available in the camera frame $\{k\}$. The data are expressed in the world frame by rotating it towards the horizontal (world) plane. The angles for this rotation are based on the (tilted) linear polynomial surface that fits all data best. Next, all three transformed marker positions are combined to find the pose of the vehicle's center. Additionally, the velocity of the vehicle is calculated using finite differences on the position.

Three different types of surfaces are used to estimate the different wheel slip parameters;

- The floor of the robotics lab, which is linoleum-based and can be considered as slippery.
- A low pile carpet, which is less slippery.
- A piece of rubber sheet, which is used as rough, nonslippery material.

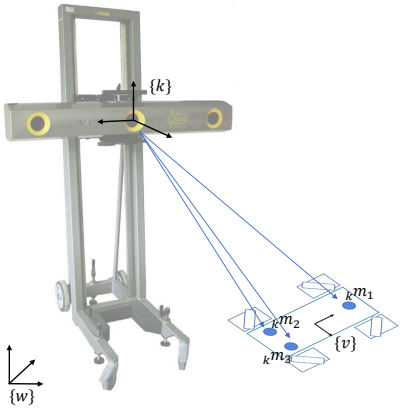

Fig. 5: The Krypton K600 system uses three cameras to accurately measure the position of each of the three LED markers (blue dots) on the vehicle.

B. Friction Coefficient Estimation

The slipping behavior on all three surfaces is investigated by performing forward and sideward motions at different speeds. All the measurements are repeated with another vehicle to check for consistency. The two friction coefficients, w_1 and w_2 as defined in our friction model (6), are estimated experimentally for all three surfaces at three different speeds over the entire speed range. We apply step inputs to move forward and sideward in both directions, e.g. applying both negative and positive wheel speeds and compare the vehicle velocity, measured by the camera, with the actual wheel speeds, measured by the wheel encoders. Our model assumes a constant traction coefficient (and thus constant force) at high amounts of wheel slip, where $|v_{\text{slip}}| > 0.1\ m/s$, and this maximal friction value w_1 can be based directly on the acceleration levels reached during extensive wheel slip. The value for w_2 is chosen heuristically for a smooth transition between the extreme values. We performed multiple experiments starting at different velocities, which can be zero, low or high and positive or negative. As the experiments showed, there is no clear distinction with respect to the starting speed of the experiment, i.e. the acceleration levels are considered to be independent from the starting speed.

There were almost no slip effects seen at the lowest speed, so we removed these ones from our measurements. At medium and high speed, a lot of wheel slip was present and Fig. 6 shows the boxplots of these results for the three surfaces for both vehicles. We performed 275 actions at high speed and 152 actions at medium speed. Although there is some spread in the acceleration (and more outliers in the case of the very slippery floor), one level of acceleration can be distinguished for every surface, with no significant differences between the forward and sideward movement, except for a slightly larger spread in the case of sideward movement. The traction coefficient as a function of the amount of wheel slip is visualized in Fig. 7 for the three different surfaces and Table II summarizes the constants found and used further on. The rubber surface

TABLE II: Summary of the constants used in the wheel slip model for three different surfaces.

Surface	$w1$ [-]	$w2$ [-]
Floor	0.093	15
Carpet	0.119	30
Rubber	0.177	30

yields the highest friction coefficient, as was expected, and only very small differences between encoder wheel speed and vehicle speed were seen. Fig. 8 compares the measurements of multiple forward and backward maneuvers on the three different surfaces at maximum speed with the simulated results based on the estimated friction coefficients for every surface and model as above and shows the good correspondence of the model with the measurements.

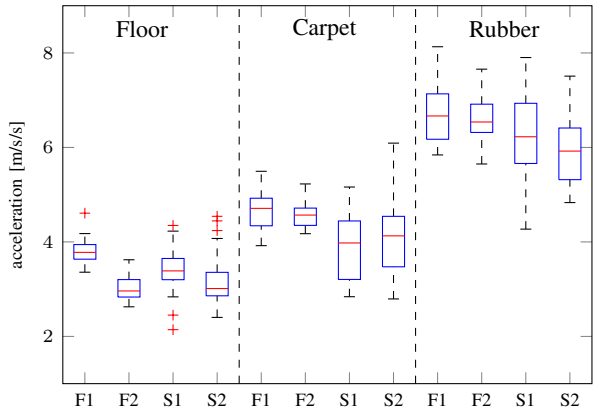

Fig. 6: Acceleration levels for three different surfaces and two maneuvers, labeled as F(orward) and S(ideward) for vehicle 1 and 2.

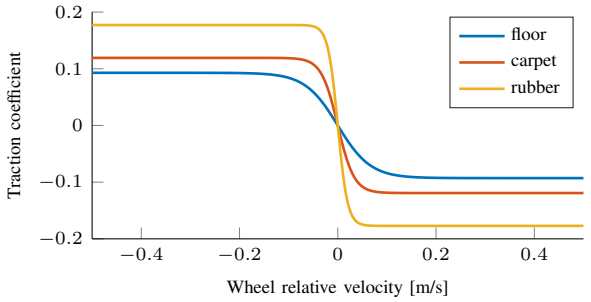

Fig. 7: Traction coefficient vs. wheel relative velocity for three different surfaces.

IV. Motion Planning

The friction model will be validated experimentally by implementing it in a motion planning problem, where we want to track a square path as closely as possible. All wheel speeds that need to be applied are calculated in advance and are applied in open loop to the vehicle at a fixed frequency.

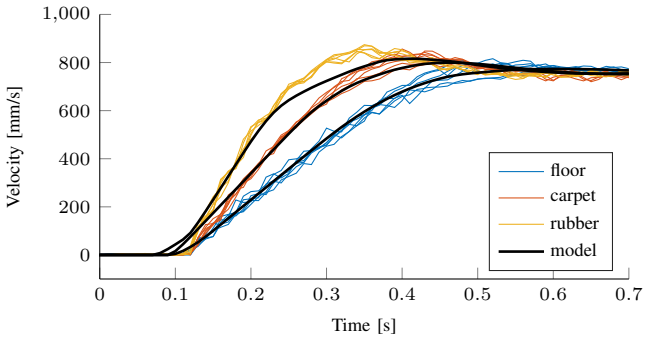

Fig. 8: Validation of the model with estimated parameters for three different surfaces.

The problem will be formulated as a constrained optimization problem and solved with Rockit, a software framework to quickly prototype optimal control problems, developed by the KU Leuven MECO research team and presented in [26].

A. Optimal Control Problem

The optimal control problem, which solves the motion planning problem, returns the four wheels speeds, $\mathbf{u}(t) = [\dot{\varphi}_1(t), \dot{\varphi}_2(t), \dot{\varphi}_3(t), \dot{\varphi}_4(t)]^\top$, that are needed to follow the square path as accurate as possible, taking into account the vehicle model with wheel slip $\mathbf{f}(\mathbf{q}(t), \mathbf{u}(t))$. The state vector includes the robot's pose with its derivative, $\mathbf{q}(t) = [x, y, \theta, v_x, v_y, \omega_z]$. We solve this as a time optimal problem, with T the total motion time, to ensure having the highest speeds possible, while the vehicle is enforced to stay within a small corridor around the square path, formally represented with a distance function dist(). In addition, there are also some boundary conditions on the states and controls, determining the vehicle's initial and final state and the orientation of the vehicle is constant at 0°. The high level optimization problem looks as follows:

$$
\begin{aligned}
\min_{\mathbf{q}(\cdot),\mathbf{u}(\cdot),T} \quad & T \\
\text{subject to} \quad & \dot{\mathbf{q}}(t) = \mathbf{f}(\mathbf{q}(t), \mathbf{u}(t)), \\
& \mathbf{q}(0) = \mathbf{q}_0, \qquad \dot{\mathbf{q}}(0) = \dot{\mathbf{q}}_0, \\
& \mathbf{q}(T) = \mathbf{q}_T, \qquad \dot{\mathbf{q}}(T) = \dot{\mathbf{q}}_T, \\
& \mathbf{u}(0) = \mathbf{u}_0, \qquad \mathbf{u}(T) = \mathbf{u}_T, \\
& \mathbf{u}_{\min} \leq \mathbf{u}(t) \leq \mathbf{u}_{\max}, \\
& \mathbf{q}_{\min} \leq \mathbf{q}(t) \leq \mathbf{q}_{\max}, \\
& \text{dist}(\mathbf{q}(t), \text{path}) \leq \epsilon, \\
& \forall t \in [0, T].
\end{aligned}
\tag{10}
$$

B. Experimental Results

The position of the vehicle while driving around the square on the most slippery floor is visualized in Fig. 9 with both the requested path and realized path. This is repeated multiple times to show the consistency of the performance. We only include the results on this very slippery surface because the improvement on the nonslippery surfaces is less pronounced,

as can be expected. Fig. 9a shows the tendency of the vehicle to drift away on the slippery surface if the wheel speeds are calculated based on the classical kinematic vehicle model. Additionally, the corners are smoothed due to unmodeled wheel slip while changing driving direction. However, applying the wheel speeds calculated with the slip model for the floor surface, results in the behavior of Fig. 9b, where a large improvement can be seen. As the actual position of the vehicle is not used to close a feedback loop, this open-loop approach cannot recover if there would be any error in the position. The consistency is way better as there is no tendency anymore to drift away and the square has been tracked more accurately, especially in the corners.

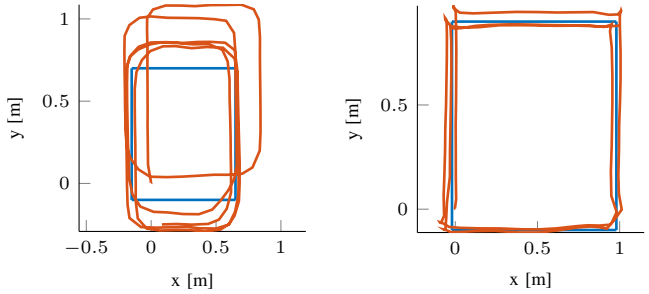

(a) Kinematic vehicle model without friction model.

(b) Dynamic vehicle model with friction model.

Fig. 9: Comparison of the resulting movement of the vehicle between the classical use of the kinematic vehicle model and the kinematic model, including the wheel slip model. All four wheels are driven independently without using position feedback to correct for deviations.

As stated in the introduction, one could improve these results even further by combining these feedforward signals with PI feedback control, where the commanded chassis velocity is calculated as the sum of the desired velocity (taking into account wheel slip) at the current time instant plus some feedback terms proportional to the current position error and, if appropriate, the time integral of this error. The amount of feedback needed to keep close to the trajectory will be significantly less if a proper wheel slip model is used.

V. Conclusion and Future Work

This paper introduced a new strategy to easily model and estimate wheel slip for two-dimensional motion of a Mecanum-wheeled vehicle. Only two parameters are required to define the traction force which is assumed to be dependent on the slip velocity. Through the use of this model in an optimal control based motion planning, the vehicle can fully exploit its omnidirectional motion capabilities, both at low speed and at the limits of maneuverability.

Possible suggestions for future work include incorporating vehicle rotation, i.e. adding the heading of the vehicle and developing a dedicated slip estimation technique, that is less depending on the quality of the (possibly expensive) camera system. This should allow for easier deployment in industrial applications with cheaper sensors.

References

[1] Y. Li, S. Dai, L. Zhao, X. Yan and Y. Shi, Topological Design Methods for Mecanum Wheel Configurations of an Omnidirectional Mobile Robot. Symmetry 2019, 11(10), 1268, 2019.

[2] G. Bayar, and S. Ozturk, Investigation of The Effects of Contact Forces Acting on Rollers Of a Mecanum Wheeled Robot. Mechatronics, 72, 102467, 2020.

[3] Robotshop. Castor Wheel. url: https://www.robotshop.com/en/29-swivel-caster-wheel.html (visited on 17/09/2021).

[4] Robotshop. Omni Wheel. url: https://www.robotshop.com/en/60mm-aluminum-omni-wheel.html (visited on 17/09/2021).

[5] Robotshop. Mecanum Wheel. url: https://www.robotshop.com/en/127mm-aluminium-mecanum-wheels-basic-rollers-2x-left-2x-right.html (visited on 17/09/2021).

[6] L. Gracia and J. Tornero, Kinematic modeling of wheeled mobile robots with slip. Advanced Robotics, 21(11), pp. 1253-1279, 2007.

[7] M. de Villiers and N. S. Tlale, Development of a Control Model for a Four Wheel Mecanum Vehicle. Journal of Dynamic Systems, Measurement, and Control, 134(1), 011007, 2011.

[8] R. L. Williams, B. E. Carter, P. Gallina and G. Rosati, Dynamic Model with Slip for Wheeled Omni-Directional Robots. In IEEE Transactions on Robotics and Automation, 18(3), pp. 285-293, 2002.

[9] F. Gustafsson, Slip-based Tire-Road Friction Estimation. Automatica, 33(6), pp. 1087-1099, 1997.

[10] K. Han, H. Kim and J. S. Lee, The sources of position errors of omni-directional mobile robot with Mecanum wheel. In IEEE International Conference on Systems, Man and Cybernetics, 2010, pp. 581-586, 2010.

[11] P.-J. Chen, S.-Y. Yang, Y.-P. Chen, M. Muslikhin and M.-S. Wang, Slip Estimation and Compensation Control of Omnidirectional Wheeled Automated Guided Vehicle. Electronics 2021, 10(840), 2021.

[12] X.-Y. Lu and J.K. Hedrick, Real-time Estimation and Compensation of Road Slip for Longitudinal Control. In Vehicle System Dynamics, 37(1), pp. 50-66, 2002.

[13] H. Dugoff, P. Fancher and L. Segel, An analysis of tire traction properties and their influence on vehicle dynamic performance. SAE Technical Paper 700377, 1970.

[14] E. Bakker, L. Nyborg and H. B. Pacejka, Tyre modeling for use in vehicle dynamics studies. SAE paper #870421, 1987.

[15] C. Canudas-de-Wit et al., Dynamic Friction Models for Road/Tire Longitudinal Interaction. Vehicle System Dynamics, 39, pp. 189-226, 2003.

[16] J.A. Cooney, W. L. Xu and G. Bright, Visual dead-reckoning for motion control of a Mecanum-wheeled mobile robot. Mechatronics, 14(6), pp. 623-637, 2004.

[17] B. Chu, Position compensation algorithm for omnidirectional mobile robots and its experimental evaluation. In Int. J. Precis. Eng. Manuf. 18, pp. 1755–1762, 2017.

[18] C. C. Ward and K. Iagnemma, A Dynamic-Model-Based Wheel Slip Detector for Mobile Robots on Outdoor Terrain. In IEEE Transactions on Robotics, 24(4), pp. 821-831, 2008.

[19] R. Van Parys and G. Pipeleers, Distributed MPC for multi-vehicle systems moving in formation. Robotics and Autonomous Systems, vol. 97C, pp. 144-152, 2017.

[20] G. Campion, G. Bastin and B. D'Andrea-Novel, Structural properties and classification of kinematic and dynamic models of wheeled mobile robots. IEEE Transactions on Robotics and Automation, 12(1), pp. 47-62, 1996.

[21] K. M. Lynch and F. C. Park, Modern Robotics: Mechanics, Planning, and Control. Cambridge University Press, pp. 517-522, 2017.

[22] L. Gracia and J. Tornero, Kinematic modeling and singularity of wheeled mobile robots. Advanced Robotics, 21, pp. 793-816, 2007.

[23] P. F. Muir and C.P. Neuman, Kinematic modeling of wheeled mobile robots. J. Robotic Syst. 4, pp. 281–329, 1987.

[24] S. Stepanyuk, R. Bruns and K. Krivenkov, Empirical lateral-force-model for forklift tires. Logistics Research, ISSN 1865-0368, Bundesvereinigung Logistik (BVL), Bremen, Vol. 10, Iss. 1, pp. 1-12, 2017.

[25] M. Abderrahim, A. Khamis, S. Garrido and L. Moreno, Accuracy and calibration issues of industrial manipulators. Industrial Robotics: Programming, Simulation and Applications, pp. 131–146, 2006.

[26] J. Gillis, B. Vandewal, G. Pipeleers and J. Swevers, Effortless modeling of optimal control problems with rockit. In 39th Benelux Meeting on Systems and Control, Elspeet, The Netherlands, 2020.